

ARTICLE OPEN



Hierarchies of Hofstadter butterflies in 2D covalent organic frameworks

David Bodesheim¹, Robert Biele¹ and Gianaurelio Cuniberti^{1,2}✉

The Hofstadter butterfly is one of the first and most fascinating examples of the fractal and self-similar quantum nature of free electrons in a lattice pierced by a perpendicular magnetic field. However, the direct experimental verification of this effect on single-layer materials is still missing as very strong and inaccessible magnetic fields are necessary. For this reason, its indirect experimental verification has only been realized in artificial periodic 2D systems, like moiré lattices. The only recently synthesized 2D covalent organic frameworks might circumvent this limitation: Due to their large pore structures, magnetic fields needed to detect most features of the Hofstadter butterfly are indeed accessible with today technology. This work opens the door to make this exotic and theoretical issue from the 70s measurable and might solve the quest for the experimental verification of the Hofstadter butterfly in single-layer materials. Moreover, the intrinsic hierarchy of different pore sizes in 2D covalent organic framework adds additional complexity and beauty to the original butterflies and leads to a direct accessible playground for new physical observations.

npj 2D Materials and Applications (2023)7:16; <https://doi.org/10.1038/s41699-023-00378-0>

INTRODUCTION

The quantum behavior of an electron moving in a two-dimensional lattice exposed to a magnetic field is a fundamental problem of solid-state physics that has been studied deeply in the 70s. By plotting for the first time the allowed energies of the electrons and varying the magnetic field, Douglas Hofstadter found the stunning form of a graph that consists of duplicates of itself, embedded infinitely deeply, and that encodes nature in such a complex but equally self-similar manner¹. This so-called Hofstadter butterfly (HB), which is shown in Fig. 1a and b, emerges from the commensurability of the magnetic and the lattice lengths when constraining a free electron onto a lattice. This effect has fascinated theoretical physicists and mathematicians over many decades^{2–10} and connects the mathematical concept of fractals with the world of physics by encoding the most exotic behaviors of quantum mechanics and topology, namely the quantum Hall effect and conductance quantization in 2D materials^{11–14}. However, the minimal magnetic field strength, B_p , for resolving HBs depends inversely on the plaquette area A_p of a lattice closed loop, such as a hexagon in a honeycomb lattice,

$$B_p = \frac{\Phi_0}{A_p}. \quad (1)$$

where, $\Phi_0 = \frac{h}{2e}$ is the magnetic flux quantum. The HB repeats itself infinitely with a period of B_p . For graphene, for instance, B_p is around 78 kT, making it inaccessible for experimental validation. Hence, the HB has served since its discovery as a physical playground of mainly theoretical interest but with no direct observation. However, in the last three decades experimental verification of the HB via artificial lattices with very large unit cells, such as moiré lattices or 2D electron gas lattices, has turned this once-theoretical issue into an active field in experimental solid-state physics nowadays^{15–26}. It was only the escamotage of artificial lattices, like moiré patterns, resulting in large plaquette

areas which enabled the first indirect experimental demonstration of HB through magnetotransport measurements.

Two-dimensional covalent organic frameworks (2D COFs), however, have not yet been at the center of such investigations and we can show that they indeed could be the first single-layered material to directly observe HBs. COFs are crystalline covalently bound organic polymers that have first been successfully synthesized in 2005²⁷. The crystalline polymers are constructed from organic building block molecules attached to each other in a regular fashion which creates a periodic and often porous structure as depicted in Fig. 1c. Due to the many available types of precursor molecules, various different structures with tunable properties are possible. As a result, COFs have gained ever since a lot of attention in the polymer and solid-state community.

Many COFs are layered materials, similar to the graphene sheets in graphite, but experimental methods have been refined to create few-layer and indeed monolayer 2D COFs^{28–35}. These are based on simpler lattice types, like honeycomb or hexagonal lattices, with usually very large unit cells. This would lead to a lower magnetic field required for the experimental validation of the HB. Additionally, it has been shown how in these materials the lattice topology itself mediates electronic and mechanical properties^{36,37}. Moreover, recent investigations of topological effects in 2D COFs showed their potential as topological materials^{38–43}. All of this makes 2D COFs interesting materials for the exploration of fractality, quantum effects and finally finding a HB at experimentally viable magnetic fields.

In Fig. 1d, the dependency of B_p on the plaquette area A_p is depicted, including known 2D COFs with honeycomb, tetragonal or square lattice structure. This shows that several COFs already exist where the HB can be measured to a great extent with experimentally achievable magnetic fields. We chose 91 T as comparison, which is twice the highest achievable continuous magnetic field ($2 \cdot 45.5 \text{ T} = 91 \text{ T}$ ⁴⁴), as the HB is symmetric in the magnetic field and consequently only half of its spectrum needs

¹Institute for Materials Science and Max Bergmann Center for Biomaterials, TU Dresden, Dresden, Germany. ²Dresden Center for Computational Materials Science (DCMS), TU Dresden, Dresden, Germany. ✉email: gianaurelio.cuniberti@tu-dresden.de

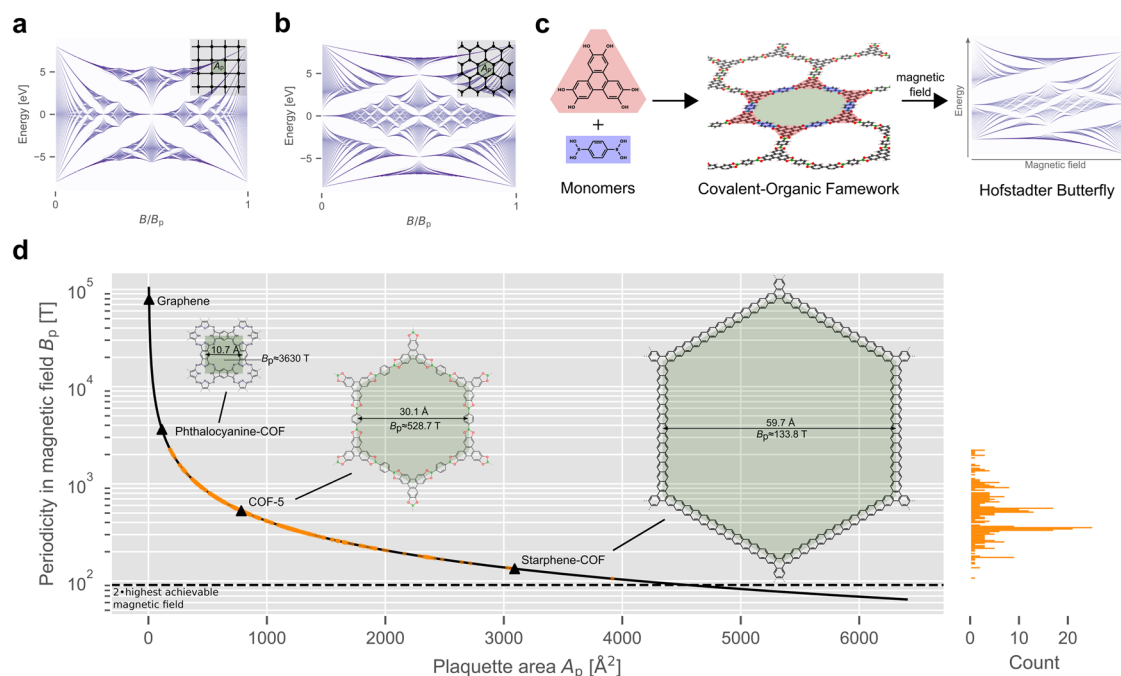


Fig. 1 From covalent organic frameworks to a measurable Hofstadter butterflies. **a, b** Application of a magnetic field to a square (honeycomb) lattice with a plaquette area A_p , marked as light green, leads to the fractal HB pattern with a period of B_p . **c** From left to right: the lattice formation of COF-5 from its tritopic (red) and linear (blue) molecular building blocks. Applying a perpendicular magnetic field to a COF leads to a HB resolved at small magnetic fields B_p . **d** Relation between the magnetic field to resolve a full HB B_p and the area of a plaquette according to Eq. (1). The dashed black line indicates twice the highest continuous magnetic field achievable to this date⁴⁴. The orange points represent experimentally known COFs with square, tetragonal and honeycomb lattices collected from the CURATED-COFs database (for details on the curation, see Supplementary Note 1)⁵⁷. The black triangles indicate graphene and the three COFs investigated in this study whose structures are shown.

to be measured. Additionally, a greater complexity and a richer phenomenon of the HB is expected due to COFs rich pore hierarchy. The HB for three different exemplary 2D COFs (shown in Fig. 1d) are calculated in the following: complex hierarchical patterns and fractal HBs can be observed at measurable magnetic fields.

RESULTS

Embedded Hofstadter butterflies

Figure 2 shows the well-known COF-5 with its three different plaquette types marked as I to III. COF-5 is the first synthesized and one of the most studied COF which has, just like graphene, a honeycomb lattice as shown in Fig. 2b²⁷. As the HB repeats itself with a period of B_p , we search for a reoccurring pattern in the calculated spectrum. In Fig. 2c, one can see such a pattern with a period of approximately 240 kT. This spectrum, however, does not resemble the HB of an equivalent honeycomb lattice (Fig. 1b) and its period is very large. A zoom into the spectrum, as shown in Fig. 2d, indicate more complex patterns and a further zoom in Fig. 2e reveals astonishingly a HB that is equivalent of the one of graphene, but only at 528.7 T. This corresponds to the B_p of the lattice plaquette I according to equation (1). To avoid confusion in the following discussion, we will call the patterns that resemble the HB of simple lattices specifically ‘HB’ and the rest of the spectrum generally ‘butterfly spectrum’.

How can we understand the formation of different patterns on the various scales of magnetic fields? As seen in Fig. 2c, the butterfly spectrum contains many different ‘ribbons’ that change with the magnetic field. We will call those ‘ribbons’ to give a clear distinction to bands in band-structure plots. This complexity arises due to the numerous electronic states that COFs have compared to simple lattices.

A zoom closer to some of the ribbons in Fig. 2d, shows that each ribbon itself contains many smaller complex features that sometimes overlap and interfere with each other and create new patterns.

A comparison with the band structure in Supplementary Fig. 2 reveals that some ribbons are based on a band-structure equivalent of a simple honeycomb lattice, while others are more similar to the one of a kagome-lattice. It is known that COF-5 has kagome-characteristic bands⁴⁵. The resulting butterfly spectrum of these kagome-like bands is similarly distorted as the one of a simple kagome-lattice HB⁶. Furthermore, a comparison of the band structure and HBs of all studied COFs in this manuscript is shown in Supplementary Fig. 5. The final zoom in Fig. 2e into the isolated ribbon at around -6.9 eV shows the honeycomb HB. This shows that the lattice type itself dictates the electronic structure and topological effects. A key difference to the HB in a simple honeycomb lattice is that HB in COF-5 is strictly speaking not repeating itself, but is distorted for higher magnetic fields due to the superposition of different periodicities.

Hierarchical patterns in 2D COFs

But why do we see a periodic pattern at ~ 240 kT in Fig. 2c for COF-5? This value does not coincide with any of the B_p values of the three plaquette types I to III in COF-5 labeled in Fig. 2a: the honeycomb lattice plaquette I, the benzene ring II and the boronic ester based five-membered ring III, with periodicities B_p of 528.7 T, 81.06 kT, and 121.9 kT, respectively. As the latter two periods have approximately a common denominator, a new periodic pattern with a bigger period at ~ 240 kT ($\approx 2 \cdot 121.9$ kT $\approx 3 \cdot 81$ kT) is visible.

To better understand the influence of multiple plaquette types on the butterfly spectrum, we next investigate a COF with four different plaquettes. This COF is based on Phthalocyanine as

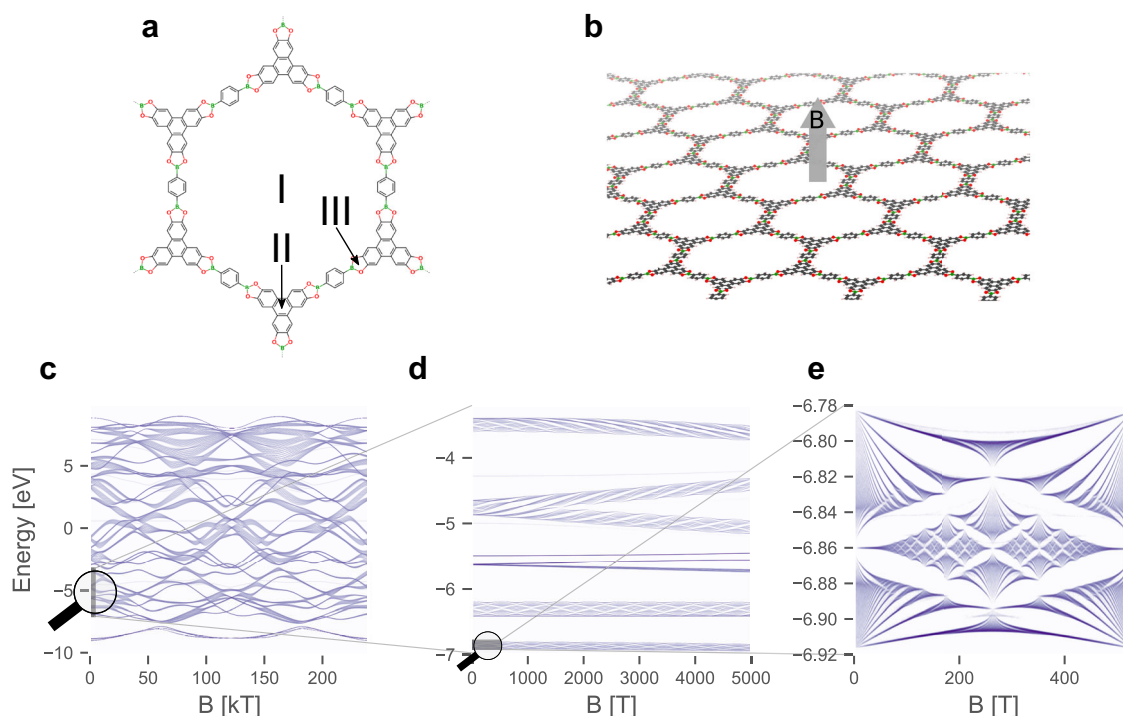


Fig. 2 Hierarchical periodic spectra for COF-5. **a** Structure of COF-5 including annotations for the largest to the smallest plaquettes (I–III). **b** Extended 2D structure of the honeycomb lattice of COF-5 with indicated applied magnetic field. **c** Butterfly spectrum from 0 to 240 kT. **d** Butterfly spectrum from 0 to 5000 T. **e** Honeycomb HB from 0 to 530 T. The intensity of the DOS in the butterfly spectra is depicted in a logarithmic scale although the colorbar was omitted for clarity.

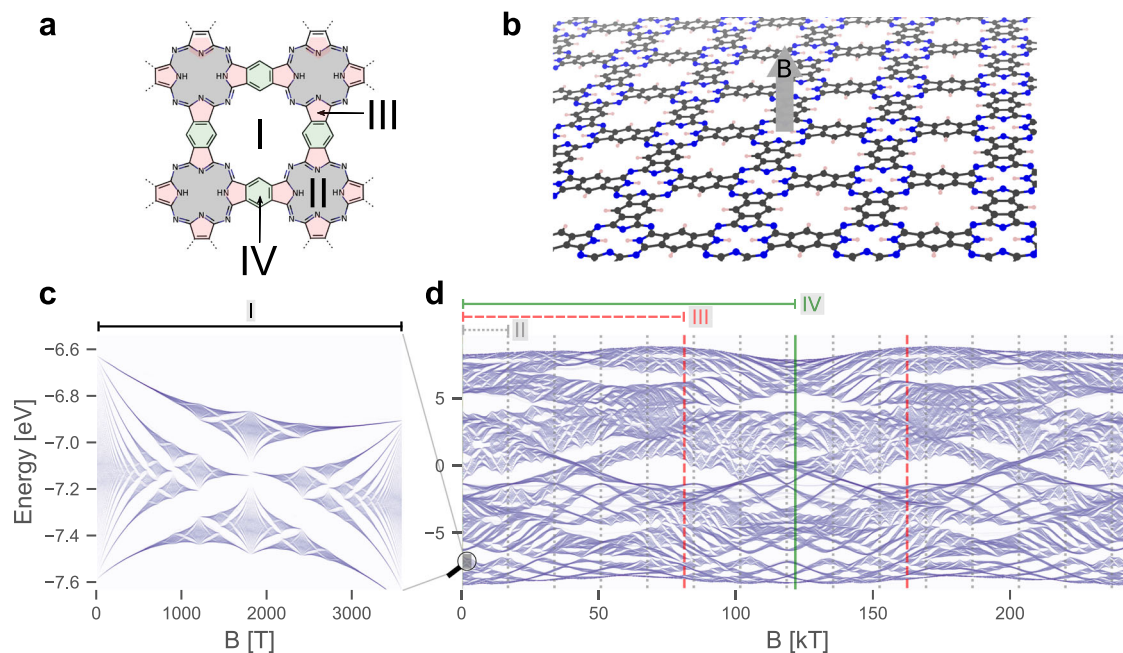


Fig. 3 Different periodicities in the butterfly spectrum shown in the example of Phthalocyanine-COF. **a** Structure of the Phthalocyanine-COF including annotations for the largest to the smallest plaquettes (I–IV). **b** Extended 2D structure of Phthalocyanine-COF including an indicated applied magnetic field. **c** HB from 0 to 3600 T. **d** Butterfly spectrum from 0 to 245 kT. The solid green lines indicate the periodicity generated by plaquette IV (121.6 kT), the dashed red line by plaquette III (81.18 kT), and the dotted gray line by plaquette II (16.92 kT). The intensity of the DOS in the butterfly spectra is depicted in a logarithmic scale although the colorbar was omitted for clarity.

shown in Fig. 3a and has a square lattice. It has been shown in previous studies that this COF has interesting topological properties, although usually investigated including a metal-center^{40,42,43}. In Fig. 3a, we depict the four different kinds of plaquettes marked as I to IV: square lattice plaquette that arises from the fused

Phthalocyanines units I, the pore inside of a Phthalocyanine unit II, the benzene ring III and the pyrrole five-membered ring IV. In Fig. 3d, we can see that similar to COF-5, there is an overlap of the periodicities of III (81.18 kT) and IV (121.6 kT) that leads to a new combined pattern with a period of ~240 kT.

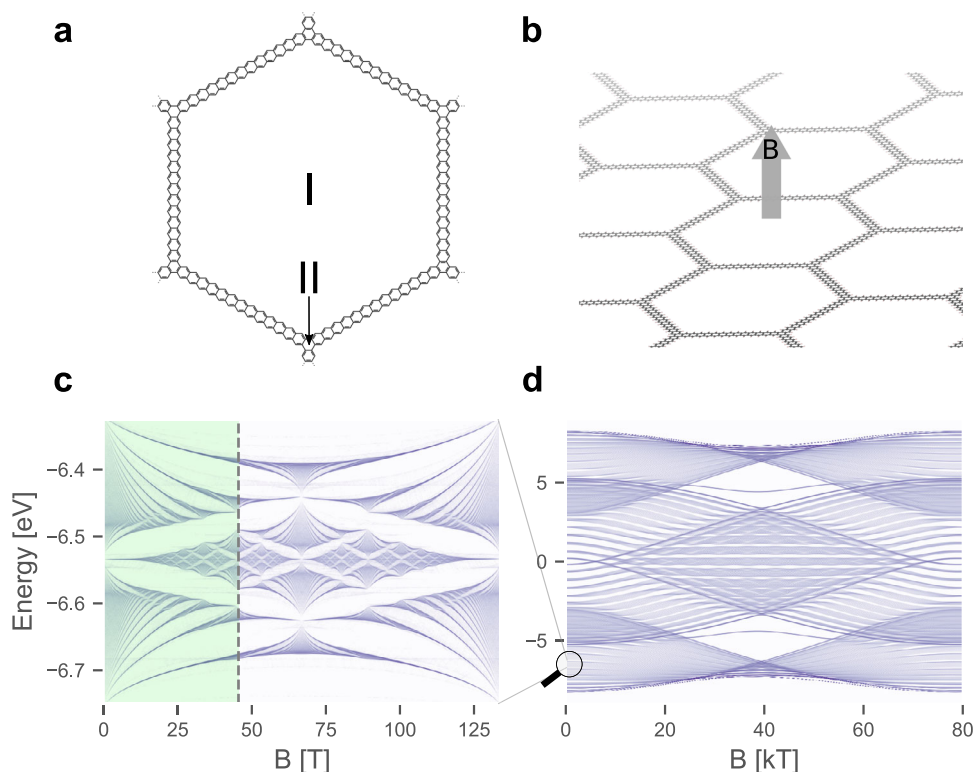


Fig. 4 Towards a measurable HB in 2D COFs with the Starphene-COF. **a** Structure of the Starphene-COF. **b** Extended 2D structure of the honeycomb lattice of the Starphene-COF including an indicated applied magnetic field. **c** HB from 0 to 134 T. The green overlay indicates the range in which the spectrum would be measurable according to the highest achievable magnetic field of 45.5 T⁴⁴. **d** Butterfly spectrum from 0 to 80 kT. The intensity of the DOS is depicted in a logarithmic scale although the colorbar was omitted for clarity.

The spectrum shows that there are patterns with different periods which are marked in the figure. For better visualization of the repeating patterns, a wider magnetic field range of the butterfly spectrum plotted in Supplementary Fig. 3. When zooming into one of the ribbons in Fig. 3d, we see as expected a HB in Fig. 3c that resembles the one of a square lattice (compare to Fig. 1a), which further shows how lattice types guides topological effects like the HB. But since the period of II is only around five times larger than I, the oscillation of II distorts the HB in Fig. 3c. From this we can see that the closer the scales of periodicities of different plaquettes are, the more they influence each other and the more distorted the HB is.

We would like to point out that the fractality and the actual HB is only created by the lattice plaquette, i.e. the biggest plaquette. The other plaquettes are only responsible for additional periodicity, but not for fractality, as shown in Supplementary Fig. 4.

Towards a measurable HB in 2D COFs

The COFs investigated so far do not have large enough unit cells to create a periodicity B_p that would be measurable in today's experiments. Hence, a COF with larger pores is required. One COF (COF-122) exists already that is close to the required unit cell size⁴⁶. However, as parts of this COF have many rotational degrees of freedom and is hence not flat, it is in our opinion not suitable for a flat monolayer material. For this reason, we propose a COF that is based on the recently reported class of Starphene molecules which are triangular molecules of fused benzene rings⁴⁷. When connected, a highly porous COF with a honeycomb lattice would result which we call Starphene-COF, as shown in Fig. 4a and b. This theoretical COF also is a fully conjugated system which should lead to a good conductivity. In the Starphene-COF, there are only two plaquette types: the honeycomb lattice plaquette I and the benzene-rings II. This leads to a period of

133.8 T for the lattice plaquette I and a period of approximately 78.68 kT for the benzene ring (II). The full butterfly spectrum up to 80 kT is depicted in Fig. 4d. In Fig. 4c, we zoom in to the magnetic field range of the smaller period and see that a HB arises that looks similar to the one of a simple honeycomb lattice in Fig. 1b. Since B_p is only 133.8 T, the HB of the Starphene-COF would be accessible to a great extent by available magnetic fields, possibly solving the quest for direct experimental verification of the HB in a single-layer 2D material in the future.

The butterfly spectrum in Fig. 4d also has some interesting properties similar to a related class of materials, graphene antidot lattices (GALs) which is graphene with periodic holes. In GALs, a typical graphene HB pattern still emerges, even though it becomes less distinct the bigger the holes in the lattice becomes. The Starphene-COF can be seen as an edge case of such a GAL, in the sense of a porous graphene which has the biggest possible hole for its repeating unit. Another feature that is known from GALs is that the band gap is being quenched with increasing magnetic field, which can be seen for the Starphene-COF at around 6 kT at 0 eV in Fig. 4d⁴⁸.

During the preparation of the manuscript, a COF with a very large pore was reported⁴⁹. We show in Supplementary Fig. 1 the corresponding HB that is resolved at 122.6 T, which is even lower than our proposed Starphene-COF. This demonstrates how the rapid advances in synthesis can provide systems to experimentally measure the HB in the near future.

DISCUSSION

We have shown that 2D COFs are promising materials for the direct experimental verification of the Hofstadter butterfly in pure 2D materials and that there are additional hierarchical patterns that are not present in HBs of simple lattices. This work might turn

this merely-theoretical issue from the 70s into an active experimental research activity nowadays and trigger the race for the first direct measurement. We found equivalents of simple lattice HB inside the complex and beautiful butterfly spectra of 2D COFs. Moreover, hierarchical structures and periodicities can be found within these spectra, due to the various pore types inside a single COF-structure, opening dimensions for more physical discoveries. Furthermore, we showed that for 2D COFs with large unit cells the magnetic field to measure a HB is small enough to be experimentally viable. 2D COFs can provide the ideal playground for the investigation of such fundamental quantum effects and the recent advances in single-layer synthesis of 2D COFs will lead in the foreseeable future to the direct observation of the Hofstadter butterfly in a single-layer 2D material.

METHODS

Calculation of the HB

A tight-binding hamiltonian was constructed from the Slater-Koster parametrization which is used in Density Functional based Tight Binding. The parameters include tabulated distance-dependent orbital-orbital interactions and respective on-site energies⁵⁰. Here, the matsci parametrization with on-site energies for the angular momentum p for the given atom and pp' hopping parameters⁵¹. The hopping was assigned according to the respective distance between the atoms. To simplify the model and the energy-spectrum, only nearest neighbor interactions were considered. With the help of the Atomic Simulation Environment (ASE) package⁵², the geometry and hamiltonian were imported into the pybinding code with which all further calculations were performed⁵³. For the geometry, only a strict 2D system was used, meaning the z -coordinates were discarded. The influence of a perpendicular magnetic field on the 2D structure was approximated with the Peierls-substitution⁵⁴:

$$t_{nm} \rightarrow t_{nm} e^{i \frac{2\pi}{\Phi_0} \int_n^m \mathbf{A}_{nm} d\mathbf{l}} \quad (2)$$

with t_{nm} as the hopping-parameter or off-diagonal elements for nearest neighbor sites n and m , Φ_0 as the magnetic flux quantum, \mathbf{A}_{nm} as the magnetic vector potential with a chosen gauge of $\mathbf{A}(x, y, z) = (B_y, 0, 0)$. The electronic density of states (DOS) for the structures with an applied perpendicular magnetic field was calculated with the in pybinding integrated Kernel Polynomial Method (KPM). In the KPM, the DOS is calculated by reconstruction from the KPM moments which are evaluated in a stochastic fashion⁵⁵. The DOS was evaluated for a 50×50 supercell and 3 random vectors for the stochastic calculation of KPM moments. Sweeping through a magnetic field range and plotting the DOS for each magnetic field, results in the shown butterfly spectra. The energy scale was centered with respect to the the minimum and maximum energy value of the butterfly spectrum. This convention for the energy scale was chosen instead Fermi level centering because the TB model only includes pp' orbitals and their occupation for more complex systems (like the Phthalocyanine-COF or COF-5) cannot be derived directly from the TB model.

Optimization of COF structures

The 2D COF-structures were obtained from optimization with Density Functional based Tight Binding calculations with the code DFTB+⁵⁶. The optimization was carried out at the Γ point with a maximum force component of $1e-06$ of the conjugate gradient algorithm. A tolerance of $1e-08$ for the self consistent cycles was chosen. As Slater-Koster parameters, the matsci parameter set was used⁵¹.

DATA AVAILABILITY

The data necessary to produce the butterfly spectrum are uploaded to https://github.com/DBodesheim/HB_pybinding upon publication.

CODE AVAILABILITY

The code necessary to produce the butterfly spectrum is uploaded to https://github.com/DBodesheim/HB_pybinding upon publication.

Received: 25 February 2022; Accepted: 10 March 2023;

Published online: 25 March 2023

REFERENCES

- Hofstadter, D. R. Energy levels and wave functions of bloch electrons in rational and irrational magnetic fields. *Phys. Rev. B* **14**, 2239–2249 (1976).
- Rammal, R. Landau level spectrum of bloch electrons in a honeycomb lattice. *J. Phys.* **46**, 1345–1354 (1985).
- Gumbs, G. & Fekete, P. Hofstadter butterfly for the hexagonal lattice. *Phys. Rev. B* **56**, 3787–3791 (1997).
- Koshino, M., Aoki, H., Kuroki, K., Kagoshima, S. & Osada, T. Hofstadter butterfly and integer quantum hall effect in three dimensions. *Phys. Rev. Lett.* **86**, 1062–1065 (2001).
- Osadchy, D. & Avron, J. E. Hofstadter butterfly as quantum phase diagram. *J. Math. Phys.* **42**, 5665–5671 (2001).
- Xiao, Y., Pelletier, V., Chaikin, P. M. & Huse, D. A. Landau levels in the case of two degenerate coupled bands:kagomé lattice tight-binding spectrum. *Phys. Rev. B* **67**, 104505 (2003).
- Nemec, N. & Cuniberti, G. Hofstadter butterflies of carbon nanotubes: pseudo-fractality of the magnetoelectronic spectrum. *Phys. Rev. B* **74**, 165411 (2006).
- Nemec, N. & Cuniberti, G. Hofstadter butterflies of bilayer graphene. *Phys. Rev. B* **75**, 201404 (2007).
- Yilmaz, F. & Oktel, M. O. Hofstadter butterfly evolution in the space of two-dimensional bravais lattices. *Phys. Rev. A* **95**, 063628 (2017).
- Ferrari, A. C. et al. Science and technology roadmap for graphene, related two-dimensional crystals, and hybrid systems. *Nanoscale* **7**, 4598–4810 (2015).
- von Klitzing, K. The quantized hall effect. *Rev. Mod. Phys.* **58**, 519–531 (1986).
- Kumar, A. et al. Integer quantum hall effect in trilayer graphene. *Phys. Rev. Lett.* **107**, 126806 (2011).
- Li, L. et al. Quantum hall effect in black phosphorus two-dimensional electron system. *Nat. Nanotechnol.* **11**, 593–597 (2016).
- Kjaergaard, M. et al. Quantized conductance doubling and hard gap in a two-dimensional semiconductor-superconductor heterostructure. *Nat. Commun.* **7**, 12841 (2016).
- Kuhl, U. & Stöckmann, H.-J. Microwave realization of the hofstadter butterfly. *Phys. Rev. Lett.* **80**, 3232–3235 (1998).
- Albrecht, C. et al. Evidence of hofstadter's fractal energy spectrum in the quantized hall conductance. *Phys. Rev. Lett.* **86**, 147–150 (2001).
- Zaric, S. et al. Optical signatures of the aharonov-bohm phase in single-walled carbon nanotubes. *Science* **304**, 1129–1131 (2004).
- Geisler, M. C. et al. Detection of a landau band-coupling-induced rearrangement of the hofstadter butterfly. *Phys. Rev. Lett.* **92**, 256801 (2004).
- Ponomarenko, L. A. et al. Cloning of dirac fermions in graphene superlattices. *Nature* **497**, 594–597 (2013).
- Dean, C. R. et al. Hofstadter's butterfly and the fractal quantum hall effect in moiré superlattices. *Nature* **497**, 598–602 (2013).
- Hunt, B. et al. Massive dirac fermions and hofstadter butterfly in a van der waals heterostructure. *Science* **340**, 1427–1430 (2013).
- Yu, G. L. et al. Hierarchy of hofstadter states and replica quantum hall ferromagnetism in graphene superlattices. *Nat. Phys.* **10**, 525–529 (2014).
- Yang, W. et al. Hofstadter butterfly and many-body effects in epitaxial graphene superlattice. *Nano Lett.* **16**, 2387–2392 (2016).
- Ni, X. et al. Observation of hofstadter butterfly and topological edge states in reconfigurable quasi-periodic acoustic crystals. *Commun. Phys.* **2**, 55 (2019).
- Huber, R. et al. Gate-tunable two-dimensional superlattices in graphene. *Nano Lett.* **20**, 8046–8052 (2020).
- Lu, X. et al. Multiple flat bands and topological hofstadter butterfly in twisted bilayer graphene close to the second magic angle. *Proc. Natl Acad. Sci. USA* **118**, e2100006118 (2021).
- Côté, A. P. et al. Porous, crystalline, covalent organic frameworks. *Science* **310**, 1166–1170 (2005).

28. Dienstmaier, J. F. et al. Synthesis of well-ordered COF monolayers: surface growth of nanocrystalline precursors versus direct on-surface polycondensation. *ACS Nano* **5**, 9737–9745 (2011).
29. Dienstmaier, J. F. et al. Isorecticular two-dimensional covalent organic frameworks synthesized by on-surface condensation of diboronic acids. *ACS Nano* **6**, 7234–7242 (2012).
30. Colson, J. W. & Dichtel, W. R. Rationally synthesized two-dimensional polymers. *Nat. Chem.* **5**, 453–465 (2013).
31. Zhong, Y. et al. Wafer-scale synthesis of monolayer two-dimensional porphyrin polymers for hybrid superlattices. *Science* **366**, 1379–1384 (2019).
32. Liu, K. et al. On-water surface synthesis of crystalline, few-layer two-dimensional polymers assisted by surfactant monolayers. *Nat. Chem.* **11**, 994–1000 (2019).
33. Li, Y., Chen, W., Xing, G., Jiang, D. & Chen, L. New synthetic strategies toward covalent organic frameworks. *Chem. Soc. Rev.* **49**, 2852–2868 (2020).
34. Li, X. et al. Partitioning the interlayer space of covalent organic frameworks by embedding pseudorotaxanes in their backbones. *Nat. Chem.* **12**, 1115–1122 (2020).
35. Ortega-Guerrero, A. et al. Multiscale modeling strategy of 2d covalent organic frameworks confined at an air–water interface. *ACS Appl. Mater. Interfaces* **13**, 26411–26420 (2021).
36. Springer, M. A., Liu, T.-J., Kuc, A. & Heine, T. Topological two-dimensional polymers. *Chem. Soc. Rev.* **49**, 2007–2019 (2020).
37. Raptakis, A., Dianat, A., Croy, A. & Cuniberti, G. Predicting the bulk modulus of single-layer covalent organic frameworks with square-lattice topology from molecular building-block properties. *Nanoscale* **13**, 1077–1085 (2021).
38. Dong, L., Kim, Y., Er, D., Rappe, A. M. & Shenoy, V. B. Two-dimensional π -conjugated covalent-organic frameworks as quantum anomalous hall topological insulators. *Phys. Rev. Lett.* **116**, 096601 (2016).
39. Jiang, W., Ni, X. & Liu, F. Exotic topological bands and quantum states in metal-organic and covalent-organic frameworks. *Acc. Chem. Res.* **54**, 416–426 (2021).
40. Pham, H. Q. & Pham-Tran, N.-N. Topological insulating phase in single-layer pentagonal covalent organic frameworks: a reticular design using metal phthalocyanine. *Chem. Mater.* **33**, 4488–4499 (2021).
41. Cui, B. et al. Realization of lieb lattice in covalent-organic frameworks with tunable topology and magnetism. *Nat. Commun.* **11**, 66 (2020).
42. Li, J., Gu, L. & Wu, R. Transition-metal phthalocyanine monolayers as new chern insulators. *Nanoscale* **12**, 3888–3893 (2020).
43. Jiang, W., Zhang, S., Wang, Z., Liu, F. & Low, T. Topological band engineering of lieb lattice in phthalocyanine-based metal-organic frameworks. *Nano Lett.* **20**, 1959–1966 (2020).
44. Hahn, S. et al. 45.5-tesla direct-current magnetic field generated with a high-temperature superconducting magnet. *Nature* **570**, 496–499 (2019).
45. Kuc, A. et al. Proximity effect in crystalline framework materials: Stacking-induced functionality in MOFs and COFs. *Adv. Funct. Mater.* **30**, 1908004 (2020).
46. Zhao, C., Lyu, H., Ji, Z., Zhu, C. & Yaghi, O. M. Ester-linked crystalline covalent organic frameworks. *J. Am. Chem. Soc.* **142**, 14450–14454 (2020).
47. Holec, J. et al. A large starphene comprising pentacene branches. *Angew. Chem. Int. Ed.* **60**, 7752–7758 (2021).
48. Pedersen, J. G. & Pedersen, T. G. Hofstadter butterflies and magnetically induced band-gap quenching in graphene antidot lattices. *Phys. Rev. B* **87**, 235404 (2013).
49. Riaño, A. et al. An expanded 2d fused aromatic network with 90-ring hexagons. *Angew. Chem. Int. Ed.* **61**, e202113657 (2021).
50. Slater, J. C. & Koster, G. F. Simplified Icao method for the periodic potential problem. *Phys. Rev.* **94**, 1498–1524 (1954).
51. Manzano, H. et al. Do cement nanotubes exist? *Adv. Mater.* **24**, 3239–3245 (2012).
52. Larsen, A. H. et al. The atomic simulation environment—a python library for working with atoms. *J. Phys. Condens. Matter* **29**, 273002 (2017).
53. Moldovan, D., Andelković, M. & Peeters, F. *pybinding v0.9.5: a Python package for tight-binding calculations*. <https://doi.org/10.5281/zenodo.4010216>. (2020).
54. Peierls, R. Zur theorie des diamagnetismus von leitungselektronen. *Z. Phys.* **80**, 763–791 (1933).
55. Weiße, A., Wellein, G., Alvermann, A. & Fehske, H. The kernel polynomial method. *Rev. Mod. Phys.* **78**, 275–306 (2006).
56. Hourahine, B. et al. DFTB+, a software package for efficient approximate density functional theory based atomistic simulations. *J. Chem. Phys.* **152**, 124101 (2020).
57. Ongari, D., Yakutovich, A. V., Talirz, L. & Smit, B. Building a consistent and reproducible database for adsorption evaluation in covalent-organic frameworks. *ACS Cent. Sci.* **5**, 1663–1675 (2019).

ACKNOWLEDGEMENTS

We acknowledge financial support from the DFG project CRC-1415 (No. 417590517). We thank Antonios Raptakis for providing the geometry-files of the COF structures.

AUTHOR CONTRIBUTIONS

D.B. performed the calculations. R.B. and G.C. supervised and guided the project. All authors contributed equally to the preparation of this manuscript.

FUNDING

Open Access funding enabled and organized by Projekt DEAL.

COMPETING INTERESTS

The authors declare no competing interests.

ADDITIONAL INFORMATION

Supplementary information The online version contains supplementary material available at <https://doi.org/10.1038/s41699-023-00378-0>.

Correspondence and requests for materials should be addressed to Gianaurelio Cuniberti.

Reprints and permission information is available at <http://www.nature.com/reprints>

Publisher's note Springer Nature remains neutral with regard to jurisdictional claims in published maps and institutional affiliations.



Open Access This article is licensed under a Creative Commons Attribution 4.0 International License, which permits use, sharing, adaptation, distribution and reproduction in any medium or format, as long as you give appropriate credit to the original author(s) and the source, provide a link to the Creative Commons license, and indicate if changes were made. The images or other third party material in this article are included in the article's Creative Commons license, unless indicated otherwise in a credit line to the material. If material is not included in the article's Creative Commons license and your intended use is not permitted by statutory regulation or exceeds the permitted use, you will need to obtain permission directly from the copyright holder. To view a copy of this license, visit <http://creativecommons.org/licenses/by/4.0/>.

© The Author(s) 2023